Journal of Neuroscience Methods 225 (2014) 90–96

Contents lists available at ScienceDirect

Journal of Neuroscience Methods

journal homepage: www.elsevier.com/locate/jneumeth

Basic Neuroscience

In vitro electrophoresis and *in vivo* electrophysiology of peripheral nerve using DC field stimulation

Roger D. Madison[a,d,*], Grant A. Robinson[a], Christian Krarup[e], Mihai Moldovan[e], Qiang Li[c,d], Wilkie A. Wilson[b,d]

[a] Surgery Department, Duke University Medical Center, Durham, NC 27710, United States
[b] Social Sciences Research Institute, Duke University Medical Center, Durham, NC 27710, United States
[c] Psychiatry Department, Duke University Medical Center, Durham, NC 27710, United States
[d] Research Service of the Veterans Affairs Medical Center, Durham, NC 27705, United States
[e] Clinical Neurophysiology Department, Neuroscience Center, Rigshospitalet, Copenhagen, Denmark

HIGHLIGHTS

- A low-voltage DC electric field can move charged substances in peripheral nerve *in vitro*.
- Substance movement varies with different compartments within the nerve.
- The same DC field *in vivo* does not damage nerve.

ARTICLE INFO

Article history:
Received 21 December 2013
Received in revised form 15 January 2014
Accepted 17 January 2014

Keywords:
Electrophoresis
Electric field
Nerve
Peroneal
Axon
Threshold tracking

ABSTRACT

Background: Given the movement of molecules within tissue that occurs naturally by endogenous electric fields, we examined the possibility of using a low-voltage DC field to move charged substances in rodent peripheral nerve *in vitro*.
New method: Labeled sugar- and protein-based markers were applied to a rodent peroneal nerve and then a 5–10 V/cm field was used to move the molecules within the extra- and intraneural compartments. Physiological and anatomical nerve properties were also assessed using the same stimulation *in vivo*.
Results: We demonstrate *in vitro* that charged and labeled compounds are capable of moving in a DC field along a nerve, and that the same field applied *in vivo* changes the excitability of the nerve, but without damage.
Conclusions: The results suggest that low-voltage electrophoresis could be used to move charged molecules, perhaps therapeutically, safely along peripheral nerves.

1. Introduction

There is a rich and detailed literature about the possible function of *endogenous* low-voltage DC-fields present in all animal tissues (for a very readable review see McCaig et al., 2005). For instance, such DC-fields have been shown to influence wound healing in the rat cornea (Song et al., 2002), and to influence the distribution of growth factor receptors and growth cones on neurons *in vitro* (Hinkle et al., 1981; Patel and Poo, 1982; Giugni et al., 1987). In addition, these DC-fields have been shown to have an *electrophoretic* influence on the distribution of charged morphogenetic determinants within the cytoplasm of eggs (Jaffe, 1966). The strength of these endogenous DC-fields is in the range of 0.1–0.5 V/cm (McCaig et al., 2005).

In the present work we have examined the possibility of applying a low-voltage electric field, 10–20 times the magnitude of those that are naturally occurring, to enhance the movement of charged molecules along a peripheral nerve. When such a field (*i.e.*, 10 V/cm) is applied to a human finger, it is easily tolerated. The results suggest that such enhanced movement is possible and could be used to manipulate how intrinsic or exogenously applied molecules of interest (*e.g.*, trophic factors or signaling molecules) are distributed within a peripheral nerve. As such, this method may prove useful as a delivery mechanism for therapeutic agents to a site of nerve injury/repair to promote axonal regeneration.

* Corresponding author at: VAMC, BLRD Service, Building 16, Room 38, 508 Fulton Street, Durham, NC 27705, United States. Tel.: +1 919 286 6956; fax: +1 919 286 6811.
E-mail addresses: madis001@mc.duke.edu (R.D. Madison), robin038@mc.duke.edu (G.A. Robinson).

0165-0270/$ – see front matter © 2014 Elsevier B.V. All rights reserved.
http://dx.doi.org/10.1016/j.jneumeth.2014.01.018

2. Materials and methods

2.1. In vitro studies

The Veterans Affairs Medical Center animal care and use committee approved all procedures. All animals were maintained in approved housing with controlled lighting and free access to food and water. Nerves were harvested either from Sprague-Dawley rats (Charles River) or HB9 transgenic mice (Strain B6.Cg-Tg(Hlxb9-GFP)1Tmj/J, Stock #005029, Jackson Laboratory, Bar Harbor, ME). All rodents (mice, 20–25 g; rats, 100–180 g) were deeply anesthetized for all surgical procedures with a mixture of ketamine, xylazine and acepromazine (50, 6 and 1 mg/kg, respectively) in normal (0.9%) saline.

The peroneal branch of the sciatic nerve was exposed and freed from connective tissue. For *in vitro-chamber* experiments (Fig. 1), the 3 cm-long rat nerve was harvested and immediately placed into either a large chamber (Fig. 1A and B) or a slide chamber (Fig. 1C). The large chamber consisted of a 4 cm circle cut from a black 96-well plate (#267342, Thermo Scientific, Rochester, NY), ground flat to remove ridges and secured into a plastic Petri dish (#430589, Corning Co., Corning, NY) that served as a moat for phosphate-buffered saline (PBS, pH 7.4). The chamber was then placed into a microscope stage adapter (QE2, Warner Instruments, Hamden, CT) with heat controller (TC-324B, Warner Instruments) and maintained at 37 °C. Walls between some wells were removed to promote even heat distribution by convection. For creating an effective DC field potential between the nerve ends, they were placed into separate PBS-filled wells spaced 10 mm apart. In between the wells, the nerve passed through silicone grease dams onto a stage created on the plate and overlaid with a pool of mineral oil. In this way, the two ends of the nerve were hydrated, yet effectively electrically isolated from each other by grease/oil except through the nerve interior.

A field potential was created using a DC power supply (Model 1611, BK Precision, Chicago, IL) and applied through two silver–silver chloride pellet electrodes (1 mm, A-M Systems, Carlsborg, WA) into PBS-filled wells adjacent to those with the nerve ends. U-shaped salt bridges (1 M KCl–1% agarose in 2 mm OD glass capillary tubes) were used to electrically couple the electrode-containing wells with the nerve-containing wells.

For recording the DC potential within the nerve, a motorized manipulandum (PiezoPatch, World Precision Instruments, Sarasota, FL) was used to position a 1 MΩ tungsten electrode connected to a Neuroprobe Model 1600 amplifier (A-M Systems, Carlsborg, WA). The electrode was placed into the middle portion of the nerve submerged in mineral oil. Due to the amplifier's internal ± 2 V DC indicator limit, output voltage was instead monitored using the unlimited output connection to an oscilloscope.

For *in vitro-microscopy* experiments, a 1.5 cm-long segment of the mouse peroneal nerve containing green fluorescent motor axons was harvested and placed onto a slide prepared for visualization by confocal microscopy (Fig. 1C). The nerve was arranged so that each end was in contact with PBS, but the central portion containing the candidate compound was immersed under mineral oil. The DC field potential was created using the same power supply as above, but delivered through PBS by silver–silver chloride wires of appropriate thickness to fit under the cover glass.

Candidate compounds for nerve electrophoresis were first screened for net charge by standard 1% agarose gel electrophoresis (Fig. 2). Glycerol (30% by weight) was added to aqueous solutions (4–10%) of each candidate and the mixture loaded into wells created in the middle of an agarose gel (#A9539, Sigma–Aldrich, St. Louis, MO). Positive, negative or neutral net charge was determined for each candidate based on its gel migration within the DC field (5–10 V/cm) over time in 130 mM Tris, 45 mM boric acid, and 2.5 mM EDTA buffer (TBE buffer, #161-0741, Bio-Rad, Hercules, CA). The following compounds produced by Molecular Probes were tested for gel mobility: 3000 MW fluoroscein dextran (3KFD; Product D3306), 3000 MW tetramethylrhodamine dextran crystals (3KTD; Product D3308), 10000 MW Alexa Fluor 594 dextran (10K594; Product D22913), 10000 MW Alexa Fluor 488 dextran (10K488; Product D22910), 10000 MW Alexa Fluor 647 dextran (10K647; Product D22914), Alexa Fluor 488 ovalbumin (OVA488; Product O34781), Alexa Fluor 594 ovalbumin (OVA594; Product O34783), Alexa Fluor 647 ovalbumin (OVA647; Product O34784). In addition, Fluoro-Gold (Fluorochrome LLC, Denver, CO) was also tested.

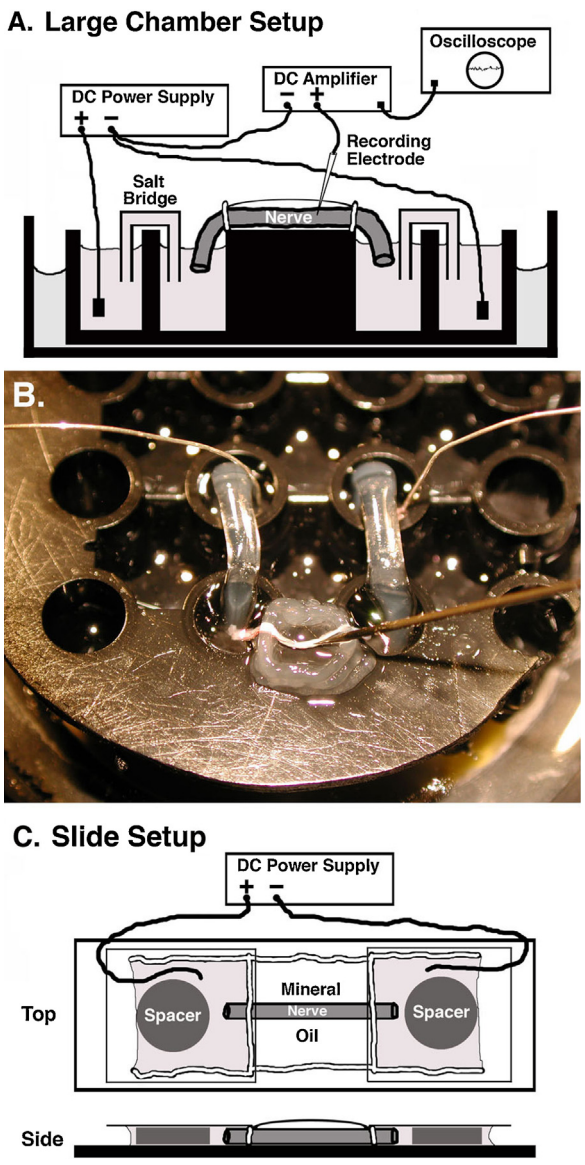

Fig. 1. Experimental conditions for *in vitro* nerve electrophoresis. The schematic for the large chamber (A) shows the nerve with a silicone grease dam around it to contain a covering of mineral oil, the salt bridges between PBS-containing wells, and the positive and negative silver–silver chloride pellet electrodes. The outermost liquid represents a heating jacket from the microscope stage adaptor. The image in (B) shows the chamber during nerve electrophoresis/recording. The center-to-center well distance is 1 cm. The schematic for the microscope slide preparation (C) has a top (upper) and a side (lower) view. The top view shows the nerve in the center of a glass slide surrounded by a silicone grease dam and covered with mineral oil. The ends of the nerve protrude through the grease into two chambers each created by overlaying a coverglass onto additional grease walls and a rubber spacer that is slightly thicker than the nerve to prevent collapse. After PBS is introduced into each chamber, the silver–silver chloride electrodes are introduced into the chambers. The side view shows this setup in cross-section at the level of the spacers.

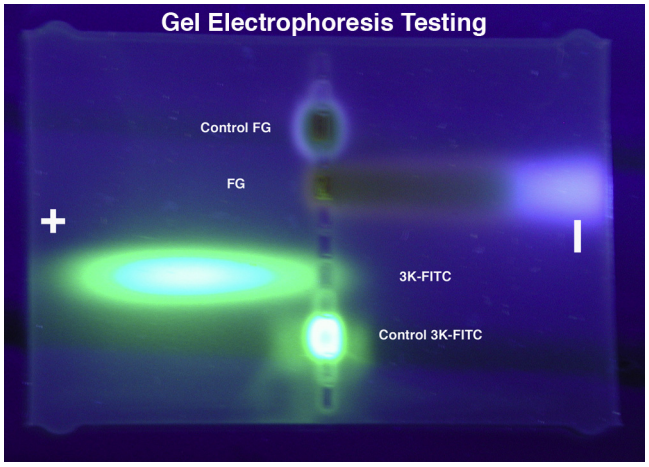

Fig. 2. Typical gel electrophoresis of candidate substances for nerve electrophoresis. Samples of Fluoro-Gold (FG, 5%) and a 3000 MW dextran labeled with fluoroscein (3K-FITC, 5%) were loaded into wells of a 1% agarose gel and exposed to a DC field (5 V/cm, 1.5 h). At the end of electrophoresis the field was stopped and identical samples were loaded into adjacent wells (Control FG and Control 3K-FITC) for the same amount of time to determine non-specific diffusion within the gel. Positively charged FG migrated toward the negative electrode and the green dextran migrated toward the positive electrode. Diffusion-only controls were limited, and showed no directionality. The lateral spread of the electrophoresis samples represents non-specific diffusion during the additional 1.5 h of Control sample monitoring.

For *in vitro-chamber* nerve electrophoresis, a candidate compound that showed gel mobility was applied to the nerve using a pulled-glass micropipette after the nerve was harvested from the animal, but prior to placement in the electrophoresis chamber. Application was either to a cut end of the nerve or into a focal crush site along the nerve. The time from harvest to the beginning of electrophoresis was routinely under 3 min. For *in vitro-microscopy* experiments, a compound was applied using a micropipette into a crush site along the nerve. All *in vitro* testing was conducted at 5–10 V/cm DC for 30 min.

After *in vitro* electrophoresis, nerves were fixed in 4% paraformaldehyde in PBS for 30 min, rinsed in PBS and then mounted in Prolong (Molecular Probes, Invitrogen, Carlsbad, CA) for viewing with a Leica TCS SP5 confocal microscope.

Movement rates for substances were determined from real-time images captured during confocal imaging or from images of histological samples stimulated for fixed times. For confocal imaging, time stamps and size bars were provided by internal software.

2.2. In vivo studies

To establish the safety of applying a low-voltage DC field to a nerve *in vivo*, motor axon electrical properties were monitored by serial nerve conduction and excitability studies in anesthetized C57BL/6J mice (Harlan, $N = 8$, adult female, 18–22 g) and nerves were harvested for histological assessment. Experimental procedures were approved by the Danish National Animal Experiment Committee. Mice were anesthetized with a subcutaneous mixture of fentanyl (0.45 mg/kg), droperidol (30 mg/kg), and midazolam (3 mg/kg) in normal saline. Detailed methods have been described previously (Moldovan et al., 2009). Briefly, after shaving the hindlimb and securing the mouse on a temperature-controlled pad (37 °C), silver–silver chloride band electrodes (Fig. 3A, 0.5 mm thick, 2 mm wide, and 30 mm long) were folded around the upper thigh (positive electrode) and ankle (negative electrode) with a center-to-center distance of ~15 mm in preparation for providing a DC field. Conductive gel (Signa Gel, Parker Laboratories, Fairfield, NJ) was applied between the skin and each electrode. Within the electric field, the peroneal nerve was stimulated using platinum needle electrodes and the evoked compound muscle action potential (CMAP) from the tibialis anterior muscle was recorded using platinum needle electrodes placed ~5 mm apart. A ground electrode was inserted subcutaneously into the opposite thigh. The amplified signal (10 Hz–6 kHz) was digitized by computer with an analog-to-digital board (NI-6221, National Instruments, Austin, TX) at a sampling rate of 10 kHz. CMAP amplitudes were measured peak-to-peak. Latencies where measured to the half peak.

The peroneal nerve was stimulated by a 0.2 ms rectangular pulse delivered from a constant current linear stimulus isolator (DS4, Digitimer, Welwyn Garden City, UK) through a cathode placed close to the nerve, proximal to the popliteal fossa. The polarizing DC current was delivered *via* a second stimulus isolator (A395, World Precision Instruments, Sarasota, FL) controlled by a digital pulse controller (Master-8, A.M.P.I., Jerusalem, Israel). The amplitude of the polarizing DC current was monitored and adjusted so that the output voltage remained within 5–10 V/cm for the entire duration of the stimulation.

Peripheral nerve excitability was monitored using QtracS© stimulation software (Institute of Neurology, London, UK). After establishing a maximal CMAP using 0.2 ms current pulses (Fig. 3B), the threshold current required to evoke a 40% maximal CMAP was automatically "tracked" using the "Multitrack" excitability sequence from the TRONDH multiple excitability protocol designed for clinical use (Kiernan et al., 2000). The integrity of the setup was first assessed by monitoring the changes in threshold current in response to brief DC currents of different polarities, *i.e.*, ensuring that hyperpolarizing current will be tracked as an increase in threshold (Fig. 3C). After establishing a "baseline" threshold of about 5 min, a DC field with a hyperpolarizing net effect was turned on for 30 min (Fig. 3D). After the DC offset, the early threshold recovery was tracked for an additional 5 min.

Although the DC field was applied using non-polarizable electrodes, a potential technical concern was that excitability in the DC field was monitored using platinum needle electrodes placed within the DC-field. Earlier studies showed that application of subthreshold polarizing currents up to 0.2 s duration as part of the routine TROND protocol in mice did not cause a substantial polarization of these electrodes (Moldovan et al., 2009). Consistent with previous observations, mouse motor axons accommodated in seconds to hyperpolarization (Boërio et al., 2009; Moldovan and Krarup, 2006). Furthermore, here we found that maintaining hyperpolarization for minutes did not cause an additional substantial sag in the threshold current (Fig. 3C and D). We therefore do not think that polarization of the electrodes played a substantial part in our measurements, possibly because the currents employed were very low.

In four mice, the peroneal nerve recovery was assessed electrophysiologically and histologically a week after DC field exposure to examine whether any axonal degeneration had occurred (Alvarez et al., 2008; Moldovan et al., 2009). Both peroneal nerves in each animal (stimulated and unstimulated) were harvested for quantitative morphometric analysis. These procedures were previously described in detail (Moldovan et al., 2009, 2011). Briefly, nerves were fixed by immersion in glutaraldehyde (2% in 0.1 M cacodylate buffer) for 24 h. The fixed nerves were then immersed in 1% osmium tetroxide in 0.1 M Sorensen's buffer, dehydrated using graded alcohols (30–100%), cleared in propylene oxide and embedded in increasing concentrations of epoxy resin until polymerized in pure epon in a heated cabinet. Cross sections (2–3 μm) of the nerve at the electrophysiological stimulation site were cut with a dry glass knife, stained with *p*-phenylenediamine, mounted, and then photographed with an Olympus BX51 microscope and DP71 camera.

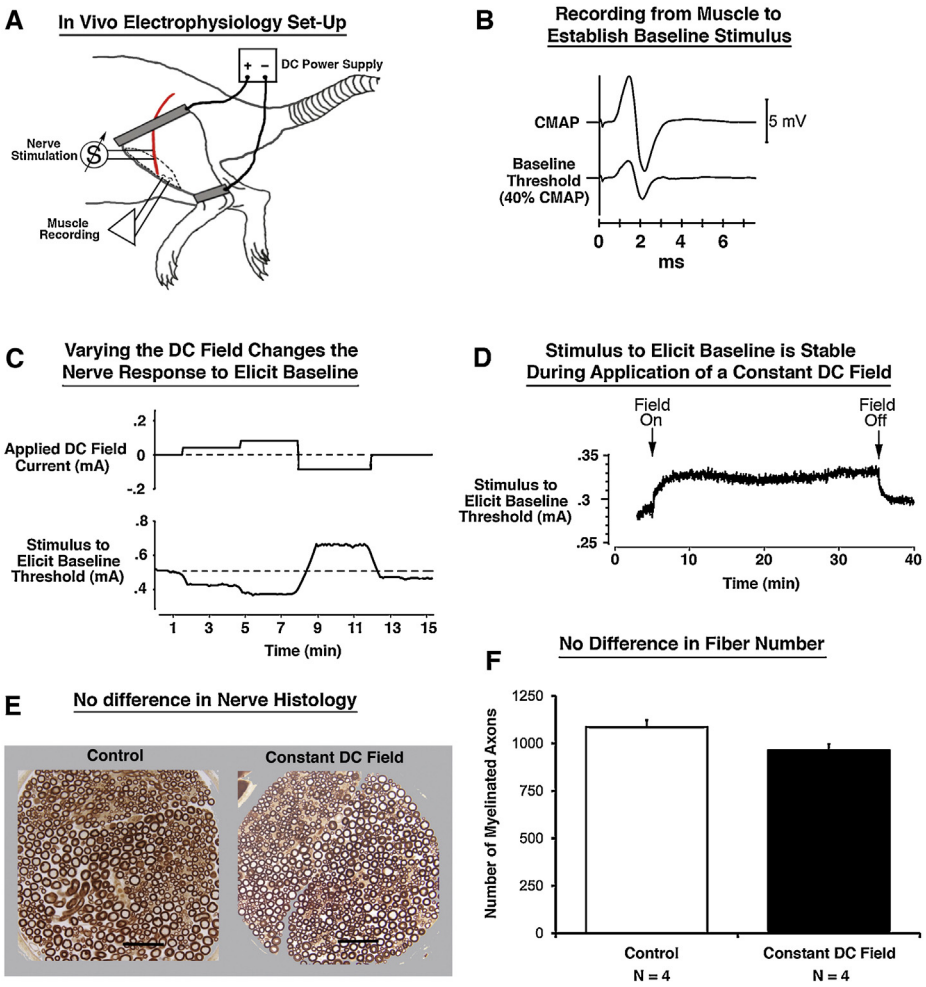

Fig. 3. Physiological and histological analyses of *in vivo* DC nerve stimulation. Panel A shows the relationship between the band electrodes (gray) for generating the DC field, the location of the peroneal nerve (red), and the stimulation and recording electrodes on the mouse hindlimb. Dotted lines outline the tibialis muscle group. Panel B shows a typical recording (upper trace) of a maximal compound muscle action potential (CMAP) in the tibialis group after directly stimulating the nerve, and the recording of the 40%-of-maximum baseline threshold potential (lower trace) used as a target to further assess the influence of DC stimulation on peroneal nerve properties. Panel C demonstrates that varying the DC field by intensity and polarity (upper trace) decreases or increases the threshold current necessary to elicit the baseline threshold potential (lower trace). Panel D shows the 30 min stability of repeatedly eliciting the baseline threshold potential by direct nerve stimulation during a constant DC field (5 V/cm, .1 mA). Panel E shows representative images of myelin-stained peroneal nerve cross sections. Compared to unstimulated control nerve, 30 min of DC stimulation caused no change in nerve fiber appearance. Scale bar = 40 μm. Panel F represents mean ± SEM fiber counts from unstimulated and stimulated nerves ($N = 4$ each). Numbers of fibers were not affected by 30 min of constant DC stimulation.

Digital images were processed using MNERVE custom morphometry software developed in MATLAB (version 2010a, MathWorks, Natick, MA). First, the total nerve area was traced from the micrographs obtained using a 40× objective. Then high magnification micrographs (100×) that included at least 10% of the total nerve area were used to automatically trace myelin rings. Fiber diameter was then calculated as the diameter of the circle having the same area as outer contours of these myelin rings. Incomplete myelin rings were not counted. The fiber density within the measured area was then used to calculate the total number of myelinated axons. Numeric results are presented as mean ± SEM.

Plotting and Wilcoxon statistical comparison of multiple measures nerve excitability was carried out using QtracS© stimulation software (Institute of Neurology, London, UK). Other Wilcoxon comparisons were carried out using SPSS (Statistical Package for the Social Sciences version 17, SPSS Inc.) with a level of <0.05 considered significant.

3. Results

3.1. In vitro studies

Candidate substances were first examined for simple diffusion and for net charge using agarose gel electrophoresis at the same field strength (V/cm) intended for nerve (Fig. 2). This allowed for proper orientation of the positive and negative electrodes relative to the nerve for moving the substances within the nerve. Preliminary experiments with different lot preparations of the same substances yielded variability in the degree of net charge (*i.e.*, migration velocity) during gel electrophoresis, indicating differences in their commercial preparation. No attempt was made to purify any of the commercial preparations.

The *in vitro*-chamber nerve preparation was then examined for the relationship between voltage applied (measured between the positive and negative pellet electrodes) and the voltage recorded from within the nerve submerged in mineral oil (measured with

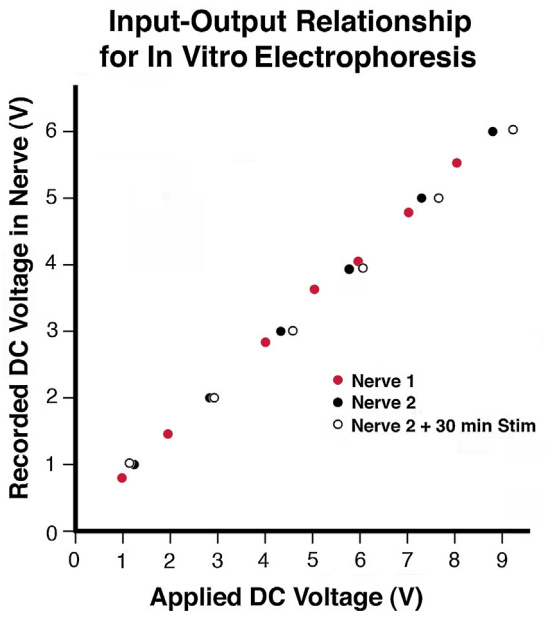

Fig. 4. Applied *versus* recorded voltage relationship for *in vitro* nerve electrophoresis. Intraneural voltage was recorded using a tungsten electrode prior to and after electrophoresis to assess how applied voltage was represented inside the rat peroneal nerve, and stability of the preparation over time. Applied voltage was only slightly diminished as recorded internally prior to electrophoresis in the two nerves examined. For the nerve examined after 30 min of electrophoresis (5 V), the relationship was still very robust, indicating that the procedure had little effect on the electric field in this preparation over time.

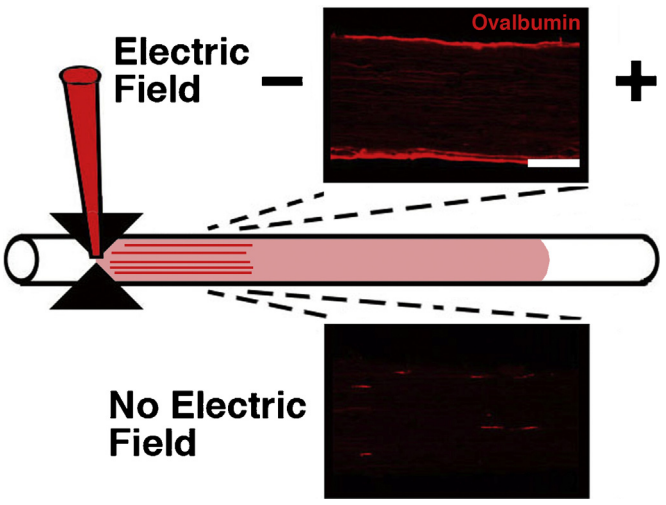

Fig. 5. Electrophoresis of a ovalbumin in mouse peroneal nerve using the *in vitro* slide preparation. Ovalbumin labeled with Alexafluor 594 was applied using a micropipette to a nerve crush site (red, middle diagram). After 30 min of a 10 V/cm electric field (top micrograph, note electrode polarity), intra-axonal protein was found ~1 mm from the application site and extra-axonal protein was seen 5–6 mm from the site. Without an electric field (duration = 30 min, lower micrograph), little protein movement was observed. Scale bar = 75 μm.

the tungsten electrode relative to the negative electrode). Fig. 4 shows this relationship for two nerves prior to electrophoresis. The ~20–40% reduction in interior voltage compared to that applied was linear for the intended voltage range and changed little after 30 min of electrophoresis. Thus, the 5–10 V/cm applied during electrophoresis in the present experiments represented a field strength of ~3–6 V/cm within the nerves.

The test substances used for chamber nerve electrophoresis were applied immediately after nerve excision using a glass micropipette to a crush site along the nerve or by application of the substance to the end face of the nerve. Both of these applications exposed the test substance to damaged nerve fibers, to the spaces around them, and to the connective tissue surrounding the fascicles. Test substances demonstrated compartmentalization within the nerves after electrophoresis. In addition to axon labeling and a more diffusely labeled endoneurium, the perineurium was routinely intensely labeled (Fig. 5). In agreement with principles of standard laboratory gel electrophoresis (*i.e.*, for DNA or protein), we also observed that the rate a substance moved within the nerve was determined by the strength of the electric field (data not shown). In addition to the strength of the field, the rate of movement was also determined by the compartment it entered. Using the *in vitro*-slide preparation, with an applied field strength of 5 V/cm for 30 min, the leading edge of Alexa-594-labeled ovalbumin traveled 5 mm within nerve fibers in rat peroneal nerve (*i.e.*, 10 mm/h, Fig. 5). The epineurial compartment appeared to have the least resistance for movement, with the protein moving extra-axonally at five times the intra-axonal speed. Diffusion alone of the protein was minimal in control nerve (Fig. 5, no electric field). In the HB9 mouse, where many motor axons contain green fluorescent protein (GFP, Fig. 6 and Supplemental Video S1), application of the same DC field moved the GFP within axons at a rate of 10 mm/h during electrophoresis using the *in vitro*-slide preparation. In contrast, the rate for the applied 3000 MW dextran was 50 mm/h in the extra-axonal compartment of the nerve (perineurium) at the same field strength, a higher rate presumably due to lower resistance in this compartment. When a ligature was placed around the HB9 peroneal nerve in the path of this movement (Fig. 6 and Supplemental Video S1), the intra-axonal dextran and GFP accumulated behind the ligature, but the perineurial dextran continued through the constricted zone. When the polarity of the electric field was reversed during electrophoresis, the movement of the test substance could also be reversed (Fig. 7 and Supplemental Video S1).

3.2. *In vivo studies*

The maximal tibialis anterior compound muscle action potential (CMAP) had a latency of 0.8 ± 0.1 ms and amplitude of 17.3 ± 5.3 mV (Fig. 3B). The stimulus artifact was negligible proving our setup (Fig. 3A) technically suitable for long term excitability monitoring.

The baseline threshold current (required to evoke the submaximal threshold CMAP) was 0.35 ± 0.08 mA. The currents necessary to induce DC fields up to 10 V/cm did not exceed 0.1 mA at the polarizing electrodes so that the smaller current flowing through the nerve could be considered subthreshold. Consistent with measurements when subthreshold polarization was applied directly at the stimulation site (Bostock et al., 1998), a depolarizing DC field was tracked as a decrease in threshold and a hyperpolarzing DC field was tracked as an increase in threshold (Fig. 3C). This strongly indicated that the fraction of the polarizing current flowing through the nerve was strong enough to alter membrane excitability.

The increase in threshold remained stable during the 30 min hyperpolarization, and showed a prompt recovery at the stimulus offset (Fig. 3D). This was the first indication that motor axon integrity was preserved. Subsequently, when re-investigated at 1 week following the DC field application, the evoked CMAP had a latency of 0.7 ± 0.1 ms and amplitude of 23.1 ± 6.6 mV, which were indistinguishable from baseline measurements (Wilcoxon $P = 0.87$ and $P = 0.37$, respectively). In addition to the CMAP we also investigated the number of myelinated fibers at the stimulated site. We found no morphological signs of Wallerian degeneration (Fig. 3E). Furthermore, the peroneal nerves had on average 1030 ± 32 myelinated axons, both on the side exposed to the DC field and the contralateral control side (Fig. 3F, Wilcoxon $P = 0.12$).

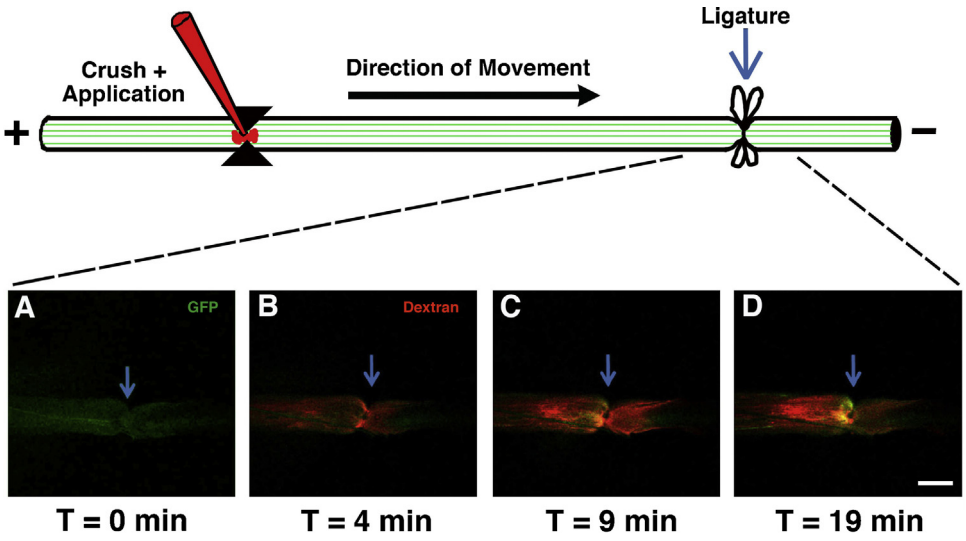

Fig. 6. Time lapse *in vitro* imaging of electrophoresis of green fluorescent protein (GFP) and a modified sugar (dextran) in a ligated mouse peripheral nerve using the *in vitro* slide preparation. The HB9 mouse peroneal nerve contains GFP-labeled motor axons (green lines, upper diagram). After application of a tetramethylrhodamine-labeled 3000 MW dextran to a nerve crush site (red pipette, left side of upper diagram), a 5 V/cm DC electric field was used to move the dextran along the nerve where it was visualized at a ligation site (blue arrow). Panel A shows only GFP-containing axons at the ligation site prior to electrophoresis. Panels B, C and D show the progressive accumulation of intra-axonal GFP and dextran at the ligation site, as well as passage of extra-axonal dextran across the ligation site. Scale bar = 250 μm.

Taken together, the DC field employed did not appear to have a neurotoxic effect *in vivo*.

4. Discussion

Here we demonstrate that application of a 5–10 V/cm DC field can move charged substances within freshly harvested peripheral nerve at a rate of ~2–10 mm/h. In fixed tissue, Swift et al. (2005) reported that 30–70 V/cm successfully moved various lipophilic dyes in fixed nerve, with average rates of 1.2 mm/h.

As there are no free electrons in these *in vitro* systems, the electric field vector created by the circuit of 'power supply and nerve' must be maintained by ions such as Cl^- or Na^+ to carry the charge. For this system, the supply of these ions is plentiful in the physiological buffer used, but we predict that any application of these principles to an *in vivo* system would necessarily result in changes to electric field strength within a nerve due to reduced ion availability in addition to other pathways for current flow with less resistance than nerve.

For each nerve preparation, the total time from excision to the end of stimulation was approximately 35 min. Based on other axon models developed to examine barrier formation after injury, this time frame is consistent with continued access to the interior of cut axons (Eddleman et al., 1998; Lichstein et al., 2000). Given

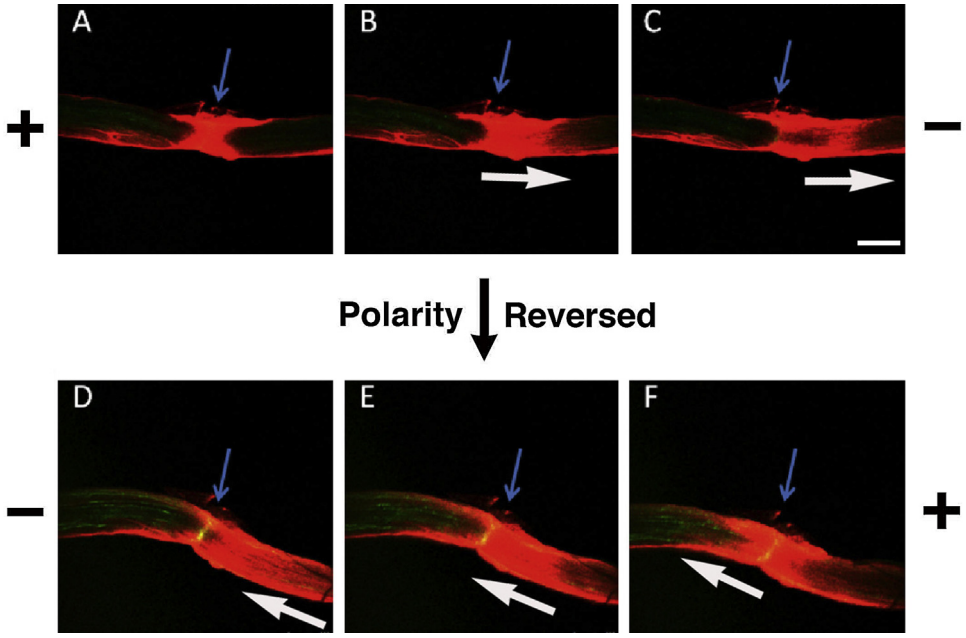

Fig. 7. Time lapse *in vitro* imaging of electrophoresis of a modified sugar (dextran) in a mouse peripheral nerve using the slide preparation. Polarity of the electrodes is shown on the sides of the panels. After micropipette application of a tetramethylrhodamine-labeled 3000 MW dextran to a nerve crush site (Panel A, blue arrow), a 5 V/cm DC electric field was used to move the dextran along the nerve toward the negative electrode (Panels B and C, white arrows). Panels B, C and D show the reversal of dextran movement when the field polarity was reversed. Scale bar = 250 μm.

the possibility that axons have not yet sealed during this course of stimulation, it is unknown whether incorporation of the various substances into the different nerve compartments (intra- and extra-axonal) was simply due to electrically enhanced diffusion similar to that described for fixed tissue (Swift et al., 2005) or included electroendocytosis, whereby an applied electric field can induce active uptake of adsorbed material through internalization of the plasma membrane (Antov et al., 2004, 2005).

Having possible therapeutic applications in mind, an important question was to what extent the 5–10 V/cm DC field applied to the whole limb induced currents that flow through the nerve. We addressed this question by monitoring the changes in motor axon threshold using automatic threshold-tracking techniques (Bostock et al., 1998). We found that, during application of the DC field there were sustained changes in motor threshold depending on the field polarity (Fig. 3C), similar to those recorded when subthreshold polarization was applied directly at the stimulation site using the same stimulator (Bostock et al., 1998; Kiernan and Bostock, 2000) or different stimulators (Moldovan et al., 2011; Moldovan and Krarup, 2004). These observations strongly suggest that the DC field employed induced currents sufficiently large to cause an altered axonal excitability. Due to safety concerns we therefore chose to test long lasting fields of polarity that caused a net hyperpolarizing effect on the axonal membrane (*i.e.*, reducing the excitability). Consistent with previous recordings using the multiple excitability tests in mice, we found that the motor axons accommodate within a second to hyperpolarization (Boërio et al., 2009; Moldovan et al., 2009). Furthermore, here we provide novel evidence that the excitability reduction can be sustained for at least 30 min (Fig. 3D). This finding ascertained an uninterrupted current flow through the nerve during the entire exposure to the hyperpolarizing DC field that might be used to move charged particles. Most importantly, the threshold change was rapidly reversible and did not cause nerve damage (Fig. 3E and F) suggesting the safety of long-term application of subthreshold hyperpolarizing fields.

With these *in vivo* results, and the *in vitro* ability to move charged substances in peripheral nerve, a therapeutic application *in vivo* may be possible. When an injured nerve is repaired, regenerating axons are likely to be influenced by molecules originating both locally and at a distance. How the specific molecules representing this influence are presented to regrowing axons is not known, but application of an appropriately polarized electric field *in vivo* could be used to move normally amphoteric proteins and other influential elements (natural or man-made) closer to the site of nerve injury to alter the normal course of regeneration. For more complex nerve injuries, a logical extension of this idea includes the possibility of applying charged therapeutic substances to a relevant final pathway downstream of the injury and then applying an electric field to move them upstream to mark the way for reinnervation back to the intended target.

Acknowledgements

Supported by the Office of Research and Development, Biological Laboratory Research and Development (BLRD), Department of Veterans Affairs (to RDM). RDM is a Research Career Scientist for the BLRD, Department of Veterans Affairs. The *in vivo* experiments were supported by the Lundbeck Foundation, the Danish Medical Research Council, the Ludvig and Sara Elsass Foundation, the Foundation for Research in Neurology, and the Jytte and Kaj Dahlboms Foundation.

Appendix A. Supplementary data

Supplementary data associated with this article can be found, in the online version, at http://dx.doi.org/10.1016/j.jneumeth.2014.01.018.

References

Alvarez S, Moldovan M, Krarup C. Acute energy restriction triggers Wallerian degeneration in mouse. Exp Neurol 2008;212:166–78.
Antov Y, Barbul A, Korenstein R. Electroendocytosis: stimulation of adsorptive and fluid-phase uptake by pulsed low electric fields. Exp Cell Res 2004;297:348–62.
Antov Y, Barbul A, Mantsur H, Korenstein R. Electroendocytosis: exposure of cells to pulsed low electric fields enhances adsorption and uptake of macromolecules. Biophys J 2005;88:2206–23.
Boërio D, Greensmith L, Bostock H. Excitability properties of motor axons in the maturing mouse. J Peripher Nerv Syst 2009;14:45–53.
Bostock H, Cikurel K, Burke D. Threshold tracking techniques in the study of human peripheral nerve. Muscle Nerve 1998;21:137–58.
Eddleman CS, Ballinger ML, Smyer ME, Fishman HM, Bittner GD. Endocytotic formation of vesicles and other membranous structures induced by Ca^{2+} and axolemmal injury. J Neurosci 1998;18:4029–41.
Giugni TD, Braslau DL, Haigler HT. Electric field-induced redistribution and postfield relaxation of epidermal growth factor receptors on A431 cells. J Cell Biol 1987;104:1291–7.
Hinkle L, McCaig CD, Robinson KR. The direction of growth of differentiating neurones and myoblasts from frog embryos in an applied electric field. J Physiol 1981;314:121–35.
Jaffe LF. Electrical currents through the developing fucus egg. Proc Natl Acad Sci 1966;56:1102–9.
Kiernan MC, Bostock H. Effects of membrane polarization and ischaemia on the excitability properties of human motor axons. Brain 2000;123:2542–51.
Kiernan MC, Burke D, Andersen KV, Bostock H. Multiple measures of axonal excitability: a new approach in clinical testing. Muscle Nerve 2000;23:399–409.
Lichstein JW, Ballinger ML, Blanchette AR, Fishman HM, Bittner GD. Structural changes at cut ends of earthworm giant axons in the interval between dye barrier formation and neuritic outgrowth. J Comp Neurol 2000;416:143–57.
McCaig CD, Rajnicek AM, Song B, Zhao M. Controlling cell behavior electrically: current views and future potential. Physiol Rev 2005;85:943–78.
Moldovan M, Alvarez S, Krarup C. Motor axon excitability during Wallerian degeneration. Brain 2009;132:511–23.
Moldovan M, Alvarez S, Pinchenko V, Klein D, Nielsen FC, Wood JN, et al. Nav1.8 channelopathy in mutant mice deficient for myelin protein zero is detrimental to motor axons. Brain 2011;134:585–601.
Moldovan M, Krarup C. Mechanisms of hyperpolarization in regenerated mature motor axons in cat. J Physiol 2004;560:807–19.
Moldovan M, Krarup C. Evaluation of Na^+/K^+ pump function following repetitive activity in mouse peripheral nerve. J Neurosci Methods 2006;155:161–71.
Patel N, Poo MM. Orientation of neurite growth by extracellular electric fields. J Neurosci 1982;2:483–96.
Song B, Zhao M, Forrester JV, McCaig CD. Electrical cues regulate the orientation and frequency of cell division and the rate of wound healing in vivo. Proc Natl Acad Sci 2002;99:13577–82.
Swift MJ, Crago PE, Grill WM. Applied electric fields accelerate the diffusion rate and increase the diffusion distance of DiI in fixed tissue. J Neurosci Methods 2005;141:155–63.